Gate voltage dependence of a single-electron transistor using the shuttle mechanism

Norihiko Nishiguchi
Department of Applied Physics, School of Engineering, Hokkaido University, Sapporo 060-8628, Japan
(Received 10 July 2001; published 14 December 2001)

The gate voltage dependence of a single-electron transistor using the shuttle mechanism in which a vibrating conductive nanoparticle carries charges between the electrodes is studied theoretically and with numerical simulations. Two types of gate voltage effect on the transport properties are demonstrated: one is direct modulation of the current via modification in the tunneling rate, giving rise to shift of $\partial I/\partial V$ peaks on the step-like current, splitting of the current steps and periodic behavior of the current with the change in gate voltage. Another is an indirect effect due to a shift in the range of the nanoparticle vibration induced by the gate voltage. The latter effect stops the shuttle mechanism at a large gate voltage, leading to the conduction gap which widens in proportion to the gate voltage.

DOI: 10.1103/PhysRevB.65.035403 PACS number(s): 73.23.Hk, 61.48.+c, 61.46.+w

I. INTRODUCTION

In recent years, electron transport coupled to nanomechanical vibrations has attracted much attention.[1–5] The pioneering work was done by Gorelik and co-workers for transport through a metal nanoparticle that vibrates between electrodes.[1,2] Over the last five years it was proposed to use chemically tailored ligand-stabilized metal nanoparticles as the building units of Coulomb blockade (CB) devices.[6–9] Gorelik *et al.* noticed that the metal nanoparticles are movable because the metal nanoparticle and electrodes are linked by elastic organic ligands, and studied theoretically the effects of nanoparticle motion on electron transport.[1,2] They showed that electrons can be carried by the nanoparticle which vibrates between the electrodes, and termed this novel transport mechanism the ''shuttle mechanism.'' The electron transport owing to the shuttle mechanism was recently observed for single-C_{60} transistors.[10] The experiment showed staircase current-voltage (I-V) characteristics as well as a strong gate-voltage dependence of the *I-V* curves. For example, the peaks in $\partial I/\partial V$ shift with change in gate voltage. Another remarkable effect of the gate voltage is that the conduction gap, which is the voltage width of the zero-conductance region, widens in proportion to the gate voltage. These apparent gate-voltage dependences of the *I-V* characteristics will provide useful techniques for current control of CB devices utilizing the shuttle mechanism. However, the modulation for the transport properties by the gate voltage and the mechanism of the conduction gap have not been properly understood from the theoretical viewpoint. In particular, the sample dependence of the conduction gap[10] has not been elucidated.

The purpose of this paper is to investigate theoretically the gate-voltage dependence of the shuttle current and to demonstrate the mechanism of the conduction gap. The outline of this paper is as follows. In Sec II, we model the system consisting of a movable nanoparticle between electrodes, and notice that the shift in mechanical equilibrium position of the nanoparticle, induced by the gate voltage, significantly affects the shuttle mechanism and relevant current. In Sec. III, we investigate how the source-drain voltage and the gate voltage affect the shuttle mechanism, taking account of the shift in the equilibrium position of the nanoparticle. In Sec. IV, we show the gate-voltage dependence of the shuttle current for symmetrically and asymmetrically applied source-drain voltage together with numerical simulations. A summary and discussion are given in Sec. V.

II. MODEL

We consider a nanoparticle linked to two electrodes by spring as shown in Fig. 1, where the mechanical equilibrium position of the nanoparticle is assumed to be on the midpoints of the electrodes. The spring arises from elastic forces in an organic ligand for a metal nanoparticle or from van der Waals forces for a C_{60} molecule bound to an electrode. The electrical resistance between the nanoparticle and the elec-

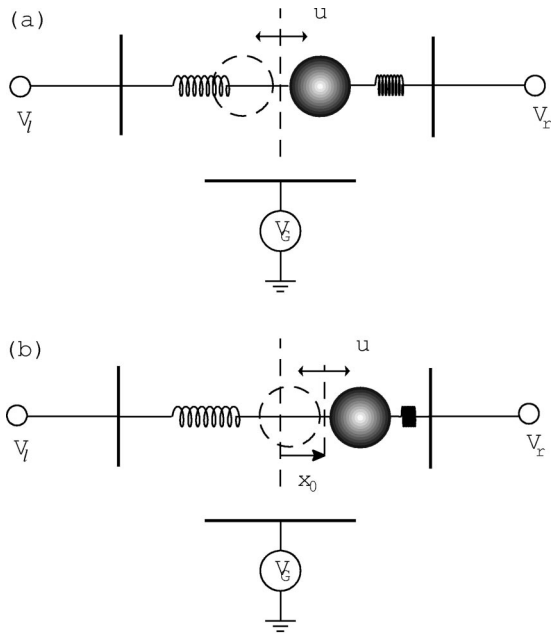

FIG. 1. Model of a movable nanoparticle linked to two electrodes with a spring. The center of nanoparticle vibrations moves from (a) the midpoint of the electrodes at $U_G=0$ for symmetrically applied source-drain voltage to (b) x_0 when $U_G\neq 0$ or asymmetrically source-drain voltage is applied.

trodes is larger than $\hbar/e^2$,[8,10] and the charging energy of the nanoparticle is larger than the thermal energy at room temperature due to the capacitance C of a nanoparticle being of the order of 0.1 aF.[8] Hence, one may assume that electrons are localized in the nanoparticle or in the electrodes and that the electron transport is due to single electron-tunneling between the nanoparticle and the electrodes even at room temperature.

The single-electron tunneling is affected by the nanoparticle motion because of the exponential dependence of the tunnel resistance on the nanoparticle displacement u.[1] The tunneling rate Γ at $T=0$ K between the nanoparticle and an electrode is given, from the golden rule, by

$$\Gamma_{n\to n'}(t)=\frac{1}{R_T C}e^{\pm u/\lambda}f(\Delta\mathcal{F}_{n\to n'}), \tag{1}$$

when the tunneling changes the number of excess electrons on the nanoparticle with respect to the electrically neutral state from n to n'. In Eq. (1), $f(x)=x\cdot\Theta(x)$ and $\Theta(x)$ is the Heaviside step function. R_T is the tunnel resistance for $u=0$, and λ is a parameter related to the attenuation of the wave function in the barrier region, which is typically to be in the range from 0.05 to 3 Å.[1] $\Delta\mathcal{F}_{n\to n'}$ is the change in electrostatic free energy of the system due to a tunnel event, given by $\Delta\mathcal{F}_{n\to n'}=\mathcal{F}(n)-\mathcal{F}(n')$, and $\mathcal{F}(n)$ is given by

$$\mathcal{F}(n)=-U_l m_l-U_r m_r+\frac{n^2}{2}+n\left[\frac{u}{\varepsilon^* L}(U_l-U_r)+\frac{U_l+U_r}{2\,\varepsilon^*}+U_{\mathrm{G}}\right], \tag{2}$$

where ε^* is the effective dielectric constant of insulating material surrounding the nanoparticle, L is the distance between the electrodes, and constant terms and the charge induced by the difference of the work functions are neglected.[11,12] The positive or negative sign of the exponent in Eq. (1) corresponds to the tunneling between the left or right electrode and the nanoparticle, and $m_{L(R)}$ is the number of electrons entered from the left(right) electrode to the nanoparticle. $U_{r,l}$ and U_{G} are dimensionless voltages defined by $U_{r(l,\mathrm{G})}=V_{r(l,\mathrm{G})}C/e$. Here $V_{l(r)}$ is the voltage at the left(right) electrode. As is apparent from Eqs. (1) and (2), the nanoparticle motion causes a significant increase or decrease in the rate of electron tunneling, and the gate voltage plays an important role in the modulation of the tunneling rate.

The electrostatic force acting on the charged nanoparticle due to the source-drain voltage as well as the mechanical restoring force will drive the nanoparticle. On the other hand, the gate voltage will not affect the nanoparticle motion, but influence the electrostatic force acting on the nanoparticle by adjusting the number of electrons of the nanoparticle through the tunneling rate as mentioned above. Due to the large mass of the nanoparticle, we may treat the center of mass motion of nanoparticle classically, and limit the motion to the longitudinal displacement of the nanoparticle relevant to electron transport. These considerations lead to the equation of motion of the nanoparticle, in the harmonic approximation for the spring

$$M_0\ddot{u}=-M_0\omega^2 u-\gamma M_0\dot{u}+en(t)\mathcal{E}, \tag{3}$$

where M_0 is the mass of nanoparticle, and ω is the natural angular frequency of nanoparticle vibrations. The electric field is given by $\mathcal{E}=-(V_r-V_l)/\varepsilon^* L$, where γ represents the rate of energy dissipation of the nanoparticle motion through coupling to loss processes such as those arising from the internal friction of ligands.

We give an overview of the shuttle mechanism in order to assess the effects of the gate voltage on the shuttle mechanism and the relevant current. Supposing that the nanoparticle is displaced by a distance over λ to the left-hand electrode for $U_l>U_r$, the tunneling rate from this electrode to the nanoparticle increases exponentially and predominates over that from the nanoparticle to the right-hand electrode. After a series of tunneling events, assume that the nanoparticle has N_e excess electrons with respect to the electrically neutral state. The charged nanoparticle will be driven to the right by the electrostatic force, and the tunneling rate from the nanoparticle to the right-hand electrode becomes dominant when the nanoparticle is displaced over λ to the right electrode. As a consequence of electron tunneling, the nanoparticle acquires N_h holes, and is then driven to the left. If the nanoparticle vibration energy produced by the electrostatic force overcomes energy dissipation, the nanoparticle will keep on vibrating and carry charges between the electrodes. The current per cycle $J=I/fe$ is given by the sum of N_e and N_h:[2]

$$J=N_e+N_h, \tag{4}$$

where N_e and N_h are functions of the voltages. From Eqs. (1) and (2),

$$N_e=\left\lfloor U_l-U_G-\frac{U_l+U_r}{2\varepsilon^*}+\frac{1}{2}\right\rfloor \tag{5}$$

$$N_h=\left\lfloor -U_r+U_G+\frac{U_l+U_r}{2\varepsilon^*}+\frac{1}{2}\right\rfloor, \tag{6}$$

where we have ignored the term proportional to u because $|u|/\varepsilon^* L\ll 1$. $\lfloor x\rfloor$ generates the nearest integer smaller than x. N_e discretely decreases in steps of unity with increasing U_G, while N_h discretely increases in steps of unity and cancels out the decrease of N_e. In general, the steps in N_h occur at different gate voltages from those in N_e. The current J will then exhibit a periodic response with respect to changes in U_G.

On the other hand, the increasing imbalance between N_e and N_h produced by the gate voltage will significantly influence the electron tunneling as well as the nanoparticle vibrations. The quantity $(e/2)(N_e-N_h)$ represents the nanoparticle charge averaged over one cycle, which vanishes only for $U_G=0$ with symmetrically applied source-drain voltage, i.e., $U_l=-U_r$. The averaged charge is, in general, finite and

the relevant electrostatic force moves the mechanical equilibrium position of the nanoparticle by x_0 from the midpoints of the electrodes as shown in Fig. 1(b). This leads to a suppression in the number of the tunnel events between the nanoparticle and the electrode from which the nanoparticle recedes because of the exponential decrease in the tunneling rate. Such an extreme suppression of the tunneling events at a large gate voltage will stop the nanoparticle vibrations. The change in gate voltage will thus not only modify the shuttle current but also terminate the shuttle mechanism. Considering these effects, we shall now analytically investigate the gate voltage dependence of the *I-V* characteristics due to the shuttle mechanism.

III. SHUTTLE INSTABILITY

Assuming that the nanoparticle vibrations depend on both the source-drain voltage $U(\equiv U_l - U_r)$ and the gate voltage U_G as we illustrated, we investigate the condition for instability of the stationary solution of Eq. (3) or that for self-excitation of the nanoparticle vibrations, based on the work by Isaccson *et al.*[2] Introducing the nondimensional displacement given by $x \equiv u/\lambda$, Eq. (3) can be rewritten as

$$\ddot{x} + \gamma \dot{x} + \omega^2 x = \frac{\Omega^2}{2} U n(t), \tag{7}$$

where

$$\Omega^2 = \frac{2e^2}{\varepsilon^* M_0 L C \lambda}. \tag{8}$$

In this work, we consider the case $\gamma/\omega \ll 1$ and $(1/\omega C R_T)(\Omega/\omega) \ll 1$, so that we may consider there to be little difference between the angular frequency of the excited nanoparticle vibrations and the natural angular frequency ω (see Appendix A). Now consider a sinusoidal nanoparticle vibration around x_0:

$$x(t) = \tilde{x}(t) \sin \omega t + x_0, \tag{9}$$

where the amplitude $\tilde{x}(t)$ varies slowly with time in comparison with ω. Substituting Eq. (9) into Eq. (7), we have

$$2\omega \dot{\tilde{x}} \cos \omega t + \gamma \omega \tilde{x} \cos \omega t + \omega^2 x_0 = \frac{\Omega^2}{2} U n(t). \tag{10}$$

Multiplying Eq. (10) by $\cos \omega t$ and averaging over a time interval which is larger than ω^{-1} and smaller than the time scale of variation of $\tilde{x}(t)$, we have

$$\frac{d\tilde{x}}{dt} = \frac{\Omega^2}{2\omega} U \langle n(t) \cos \omega t \rangle - \frac{1}{2} \gamma \tilde{x}. \tag{11}$$

$\langle \cdots \rangle$ denotes the time averaging. The shift x_0 is related to the charge by the following equation:

$$x_0 = \frac{\Omega^2}{2\omega^2} U \langle n(t) \rangle, \tag{12}$$

which is also derived from Eq. (10). Defining vibrational energy E in units of $M_0 \omega^2 \lambda^2/2$ by $E = \tilde{x}^2$, it obeys the following equation, which is derived from Eq. (11):

$$\frac{1}{\omega} \frac{dE}{dt} = U \frac{\Omega^2}{\omega^2} W(E) - \frac{\gamma}{\omega} E, \tag{13}$$

where

$$W(E) = \sqrt{E} \langle n(t) \cos \omega t \rangle. \tag{14}$$

The first term on the right-hand side (RHS) of Eq. (13) denotes the energy pumped by the electrostatic force and the second term the energy dissipation. The first term increases with increasing U, and the nanoparticle will start to oscillate when the first term predominates over the second one at a certain voltage. Then we have the condition for the critical voltage U_C of self-excitation of the nanoparticle vibrations

$$U_C \frac{\Omega^2}{\omega^2} W'(0) = \frac{\gamma}{\omega}. \tag{15}$$

The pumped energy can be formulated in terms of the probability P_n that the nanoparticle has n electrons. Considering that P_n correlates with the nanoparticle motion (9), P_n is a function of E and phase ϕ of the nanoparticle vibrations, which is given by

$$P_n(\phi, E) = \pi \left\langle \delta_{n,n(t)} \delta\left(\sin \frac{1}{2} (\omega t - \phi) \right) \right\rangle, \tag{16}$$

which obeys the following master equation:[2]

$$\frac{dP_n}{d\phi} = -[\Gamma_E^+(n) + \Gamma_E^-(n)] P_n + \Gamma_E^+(n-1) P_{n-1} + \Gamma_E^-(n+1) P_{n+1}. \tag{17}$$

The tunneling rates per cycle $\Gamma_E^{\pm}$ to change the electron number from n to $n \pm 1$ are given by

$$\Gamma_E^+(n) = \nu_R e^{-x} f\left(U_l - n - \frac{1}{2} - \tilde{U}_G \right) + \nu_R e^{x} f\left(U_r - n - \frac{1}{2} - \tilde{U}_G \right), \tag{18}$$

$$\Gamma_E^-(n) = \nu_R e^{x} f\left(-U_r + n - \frac{1}{2} + \tilde{U}_G \right) - \nu_R e^{-x} f\left(-U_l + n - \frac{1}{2} + \tilde{U}_G \right). \tag{19}$$

In Eqs. (18) and (19), we introduce $\tilde{U}_G$ and ν_R, for convenience, defined by

$$\tilde{U}_G = U_G + \frac{U_l + U_r}{2\varepsilon^*} \tag{20}$$

and

$$\nu_R=[CR_T\omega]^{-1}. \tag{21}$$

$W(E)$ can be rewritten, by using Eq. (16), as

$$W(E)=\frac{\sqrt{E}}{2\pi}\int_0^{2\pi} q(\phi,E)\cos\phi d\phi, \tag{22}$$

where

$$q(\phi,E)=\sum_n nP_n(\phi,E). \tag{23}$$

The equation governing q is derived from the master equation (17) as follows:

$$\frac{dq}{d\phi}=\sum_n [\Gamma_E^+(n)-\Gamma_E^-(n)]P_n. \tag{24}$$

Equation (24) can be written in closed form for specific voltages, and the resultant equation depends on the symmetry of the applied voltages. We should consider two representative cases: (a) the symmetric case where $U_l=-U_r=U/2>0$, and (b) the asymmetric case where $U_l=U>0$ and $U_r=0$.

A. Symmetric case: $U_l=-U_r=U/2>0$

For specific combinations of U and U_G, i.e., $U=2m+1$ and $U_G=l$, or $U=2m$, and $U_G=l+\frac{1}{2}$, where l is an integer, and m is 0 or a positive integer for the former case and a positive integer for the latter case, Eq. (24) becomes

$$\frac{dq}{d\phi}=-\nu_R[2(q+U_G)\cosh x+(U-1)\sinh x]. \tag{25}$$

The charge q is derived for small E from a power series in $\sqrt{E}$:

$$q=-U_G+\frac{1-U}{2}\tanh x_0+\nu_R\frac{1-U}{\cosh x_0}\frac{1}{1+4\nu_R^2\cosh^2 x_0}$$
$$\times(2\nu_R\cosh x_0\sin\phi-\cos\phi)\sqrt{E}+O(E). \tag{26}$$

The first two terms on the right-hand-side of Eq. (26) denote the static part of the charge, due to the presence of the gate voltage and to the shift in the vibration center. The shift also affects the amplitude and phase of the oscillatory part of q. Introducing a phase θ defined by

$$\tan\theta=2\nu_R\cosh x_0, \tag{27}$$

q is expressed as

$$q=-U_G+\frac{1-U}{2}\tanh x_0+2\nu_R^2(U-1)\frac{\cos\theta}{\tan\theta}\cos(\phi+\theta)\sqrt{E}$$
$$+O(E). \tag{28}$$

θ increases from $\tan^{-1}(2\nu_R)$ toward $\pi/2$ with increasing $|x_0|$, giving rise to the phase shift as well as a significant decrease of the amplitude. They remarkably diminish the pumped energy as shown below, and therefore the dependence of x_0 on the gate voltage is a key factor for the condition for self-excitation of the nanoparticle vibrations.

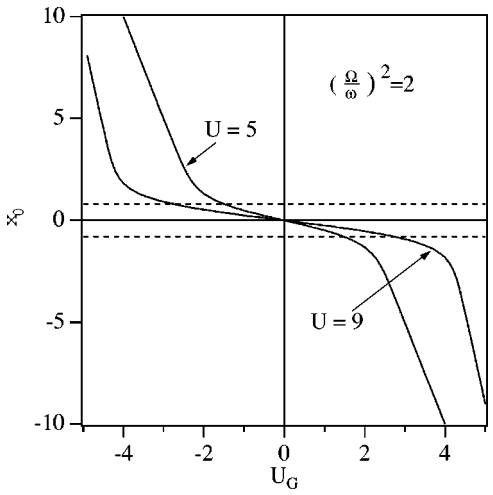

FIG. 2. The shift x_0 of nanoparticle vibration center versus the gate voltage for a symmetrically applied source-drain voltage $U=5$ and 9 where $(\Omega/\omega)^2=2$. The dashed lines denote $|x_0|=0.8$.

Putting $q(E=0)=\langle n(t)\rangle$ in Eq. (12), we have the equation for x_0,

$$x_0=-\frac{\Omega^2}{2\omega^2}U\left(U_G+\frac{U-1}{2}\tanh x_0\right). \tag{29}$$

Obviously, $x_0=0$ at $U_G=0$, and x_0 is approximated by

$$x_0=-\frac{2U_G}{U-1} \tag{30}$$

for $|U_G|\ll\frac{1}{2}(U-1)$. In contrast, x_0 is approximated for $|U_G|\gg\frac{1}{2}(U-1)$ by

$$x_0=-\frac{\Omega^2}{2\omega^2}U\left(U_G\mp\frac{U-1}{2}\right), \tag{31}$$

where the minus(plus) sign is for positive(negative) U_G. Thus, the gate voltage dependence of x_0 of the former case is quite different from that of the latter. Figure 2 plots x_0 versus U_G at $U=5$ and 9 for $\Omega^2/2\omega^2=1$,[13,14,17] showing clearly the gate voltage dependence in each voltage region and quick transitions from Eq. (30) to Eq. (31) at $|U_G|\approx(U-1)/2$. The nonlinear behavior of the gate voltage dependence of x_0 becomes clearer for larger $\Omega^2/2\omega^2$.

$W(E)$ is expected to show distinct behavior, correspondingly to that of x_0, with respect to the gate and the source-drain voltages. Substituting Eq. (26) into (22), we have

$$W(E)=\alpha E+\beta E^2+O(E^3), \tag{32}$$

where

$$\alpha=\frac{1}{2}\frac{\nu_R(U-1)}{\cosh x_0(1+4\nu_R^2\cosh^2 x_0)}, \tag{33}$$

$$\beta=\frac{1}{4}\frac{\nu_R(U-1)}{\cosh^3 x_0}\left[\frac{\sinh^2 x_0}{1+\nu_R^2\cosh^2 x_0}-\frac{\frac{7}{4}\cosh^2 x_0-1}{1+4\nu_R^2\cosh^2 x_0}+\frac{\cosh^2 x_0}{(1+4\,\nu_R^2\cosh^2 x_0)^2}\right]. \tag{34}$$

In the region $|U_G|\ll\frac{1}{2}(U-1)$ or, equivalently, $|x_0|\ll 1$,

$$U\frac{\Omega^2}{\omega^2}\alpha\approx\frac{\Omega^2}{\omega^2}\frac{U(U-1)}{2}\frac{\nu_R}{(1+4\nu_R^2)}\left(1-\frac{1}{2}\frac{1+12\nu_R^2}{1+4\nu_R^2}x_0^2\right). \tag{35}$$

This parabolically increases with increasing U and decreases with increasing $|x_0|$ or $|U_G|$. If the following condition is satisfied for certain voltages U_1 and $U_2(=U_1+2)$:

$$U_1\frac{\Omega^2}{\omega^2}\alpha_1<\frac{\gamma}{\omega}<U_2\frac{\Omega^2}{\omega^2}\alpha_2, \tag{36}$$

the critical voltage U_C for the self-excitation of the nanoparticle vibrations should be found within the region (U_1,U_2). Obviously from Eq. (35), an increase of the gate voltage raises the critical voltage U_C, because the voltage region (U_1,U_2) needs to rise complimentarily so that the relation Eq. (36) holds.

In contrast, for $|U_G|\gg\frac{1}{2}(U-1)$ or $|x_0|\gg 1$, the pumped energy becomes

$$U\frac{\Omega^2}{\omega^2}\alpha=\frac{\Omega^2}{\omega^2}\frac{1}{\nu_R}U(U-1)\exp\left[-\frac{3\Omega^2}{2\omega^2}U\left(|U_G|-\frac{U-1}{2}\right)\right]. \tag{37}$$

The slope of the pumped energy exponentially decays with increasing U or $|U_G|$, and almost vanishes at large U or $|U_G|$. The self-excitation of nanoparticle vibrations is not expected in the voltage region in question.

In order to investigate the pumped energy in the intermediate voltage region, we numerically examine the source-drain voltage dependence of the pumped energy, putting $U_G=\frac{1}{2}(U-1)+\delta$. Figure 3 plots $U(\Omega/\omega)^2\alpha$ versus U for $(\Omega/\omega)^2=2$ and $\nu_R=0.1$,[13] for example. The curve for $\delta=0$ monotonically increases and becomes of the order of unity, and then the condition (36) for the nanoparticle vibration excitation is expected to be fulfilled at some magnitude of U. On the other hand, the curves for $\delta\geqslant 1$ have peaks and exponentially decay with increasing U. Even the largest peak ($\delta=1$) is minuscule, and the peak becomes small with increasing $(\Omega/\omega)^2$ or decreasing ν_R. Although the self-excitation of the nanoparticle vibrations is anticipated for $\delta\geqslant 1$, it is limited to very small γ within the narrow source-drain voltage range of the peak region. From these results, we may conclude, for the entire range of U, that a critical gate voltage $U_{G,C}$ exists within the region $[(U-1)/2,(U+1)/2]$, and the nanoparticle vibrations will start at $U_{G,C}$ when decreasing U_G from $(U+1)/2$. For negative U_G, $U_{G,C}$ lies within the region $[-(U+1)/2,-(U-1)/2]$ and the vibrations will start when increasing U_G from $-(U+1)/2$.

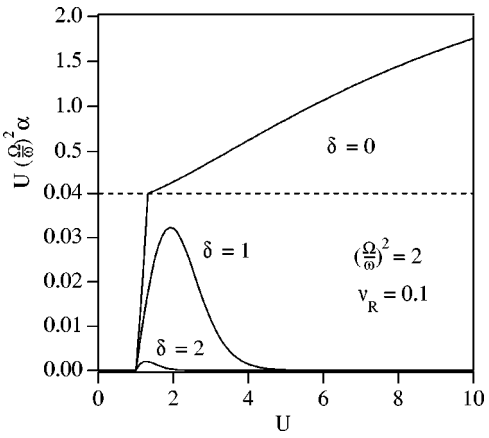

FIG. 3. The slope of the pumped energy versus U. The three curves correspond to the gate voltage given by $U_G=(U-1)/2+\delta$.

In spite of the above result, the nanoparticle might keep on vibrating for $U_G\geqslant(U+1)/2$, once the vibrations occurred when raising U_G from $(U-1)/2$. This is possible for a case of $W''(0)>0$.[2] Figure 4 shows the contour plot of $W''(0)$ in the $(\nu_R,|x_0|)$ plane. The shaded region denotes the negative curvature of W at $E=0$, which is limited to the region $\nu_R>0.3$ and $|x_0|<0.8$. As shown in Fig. 2, $|x_0|$ exceeds 0.8 for $|U_G|\geqslant(U-1)/2$, and in this case the curvature becomes always positive for $U_G\geqslant(U+1)/2$, irrespective of the magnitude of ν_R. This means not only that nanoparticle vibrations are possible for $U_G\geqslant(U+1)/2$ but also that the dynamics of the nanoparticle shows hysteretic behavior with change in gate voltage.

In order to find another critical gate voltage when raising the gate voltage from $(U-1)/2$, we examine the following equality with $\delta\geqslant 0$:

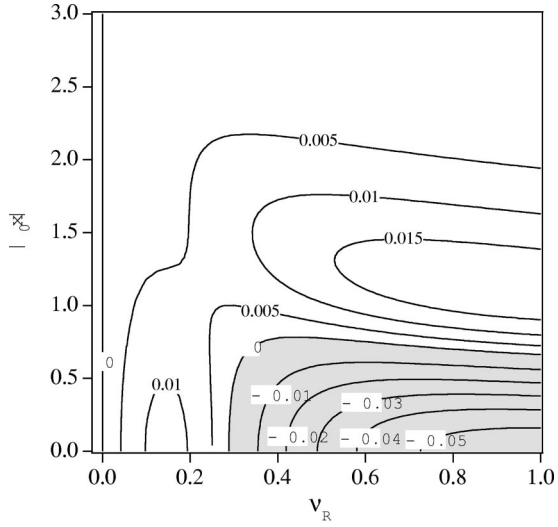

FIG. 4. Contour plot of $W''(0)$ in the $(|x_0|,\nu_R)$ plane. The shaded region denotes the negative curvature of W at $E=0$.

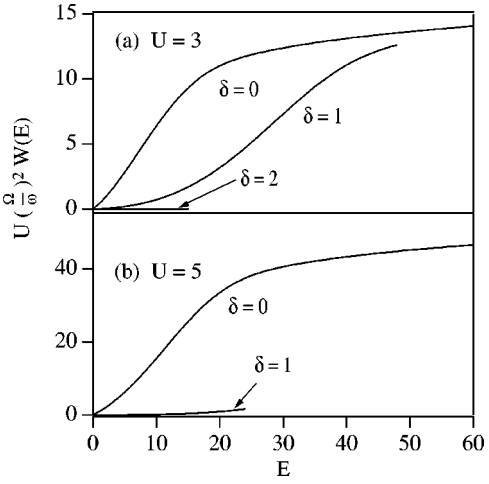

FIG. 5. The pumped energy versus E for (a) $U=3$ and (b) $U=5$. The gate voltage is given by $U_G=(U-1)/2+\delta$, where $\delta=0$, 1 and 2. The range of E and the resultant pumped energy are limited by the shift x_0 and the width of the electrodes.

$$U\frac{\Omega^2}{\omega^2}W(E)=\frac{\gamma}{\omega}E. \tag{38}$$

$W(E)$ is essentially equal to the area enclosed by the trajectory of q versus nanoparticle position [the limit cycle of $n(t)$], and $\sqrt{E}$ or the amplitude limits the region of the nanoparticle vibrations. Applying the gate voltage, the region moves to $[-\sqrt{E}+x_0,\sqrt{E}+x_0]$ as we have discussed. However, the nanoparticle is actually confined between the electrodes, and the vibration region should be limited to this space. Then the amplitude is capped by $\sqrt{E}<L/2\lambda-|x_0|$, and the shift x_0 is also limited to $|x_0|<L/2\lambda$ for the same reason. Obviously the increase of $|x_0|$ toward this limit severely narrows the vibration region, diminishing the pumped energy. Figure 5 shows the capped pumped energy versus E for $\delta=0$, 1, and 2 for (a) $U=3$ and (b) 5 with $(\Omega/\omega)^2=2$ and $\nu_R=0.1$, for example. In the experimental situation of a C_{60} single electron transistor,[10] $L/2\lambda$ is of the order of 10 according to the work function.[14] In contrast to the curve for $\delta=0$ in Fig. 5(a), the curves for $\delta\geqslant 1$ are terminated and small due to the restriction on the vibration region. In particular, the curve for $\delta=2$ is negligible. This tendency becomes clearer with increasing U, as shown in Fig. 5(b). The vibration center moves further for larger $(\Omega/\omega)^2$ or U, and then the pumped energy, even for $\delta=1$, becomes negligibly small for $U=5$. To conclude, the nanoparticle vibrations will stop while raising U_G from $(U-1)/2$ to $(U+1)/2$, except for small source-drain voltages U. Then, apart from the low-voltage region of U, we have a critical gate voltage for the nanoparticle vibrations within the voltage region $[(U-1)/2,(U+1)/2]$ when U_G is raised from $(U-1)/2$.

From the considerations above, the critical gate voltages for the nanoparticle vibrations stay within the range $[(U-1)/2,(U+1)/2]$ or $[-(U+1)/2,-(U-1)/2]$ due to the similar argument for negative U_G, and hysteretic behavior with the change in the gate voltage is anticipated. This condition on the voltages leads to the restriction on the electron numbers carried by the nanoparticle. From Eqs. (5) and (6), the numbers of electrons and holes should become

$$N_e=\left\lfloor\frac{U}{2}-U_G+\frac{1}{2}\right\rfloor\geqslant 0, \tag{39}$$

$$N_h=\left\lfloor\frac{U}{2}+U_G+\frac{1}{2}\right\rfloor\geqslant 0. \tag{40}$$

These restrictions lead to a significant modulation in the I-V characteristics with the gate voltage, as shown below.

B. Asymmetric case

Putting $U_l=U$ and $U_r=0$, the equation for q is derived for $\tilde{U}_G=l+\frac{1}{2}$ and $U=m$, where l and m are integers, and $m>0$, Eq. (24) becomes

$$\frac{dq}{d\phi}=\nu_R\left[-2\left(q+\tilde{U}_G-\frac{1}{2}\right)\cosh x+(U-1)e^{-x}\right]. \tag{41}$$

The solution of Eq. (41) for small E is given by

$$q=-\tilde{U}_G+\frac{U}{2}+\frac{1-U}{2}\tanh x_0+\nu_R\frac{1-U}{\cosh x_0}\frac{1}{1+4\nu_R^2\cosh^2 x_0}$$
$$\times(2\nu_R\cosh x_0\sin\phi-\cos\phi)\sqrt{E}+O(E), \tag{42}$$

which is the same as Eq. (26) for the symmetric case at least up to $O(E^{3/2})$ except for the offset by $U/2$. Then the pumped energy becomes the same as Eq. (32) for the previous case. The shift x_0 is given by the following equation:

$$x_0=\frac{\Omega^2}{2\omega^2}U\left[-\tilde{U}_G+\frac{U}{2}-\frac{U-1}{2}\tanh x_0\right], \tag{43}$$

and is approximated, for $|\tilde{U}_G-U/2|\ll\frac{1}{2}(U-1)$ or $|x_0|\ll 1$, by

$$x_0=\frac{2}{U-1}\left[-\tilde{U}_G+\frac{U}{2}\right]. \tag{44}$$

On the other hand, for $|\tilde{U}_G-U/2|\gg\frac{1}{2}(U-1)$ or, separately, for $\tilde{U}_G\ll\frac{1}{2}$

$$x_0=\frac{\Omega^2}{2\omega^2}U\left[-\tilde{U}_G+\frac{1}{2}\right] \tag{45}$$

or for $U-\frac{1}{2}\ll\tilde{U}_G$,

$$x_0=\frac{\Omega^2}{2\omega^2}U\left[-\tilde{U}_G+U-\frac{1}{2}\right]. \tag{46}$$

In these voltage regions, $|x_0|\gg 1$. Figure 6 plots x_0 versus $\tilde{U}_G$ for $U=5$ and 9, showing rapid changes of these gate voltage dependences similar to those as seen in the symmetric case.

The behaviors of the pumped energy are essentially the same as those for the previous case. For $|\tilde{U}_G-U/2|\ll\frac{1}{2}(U$

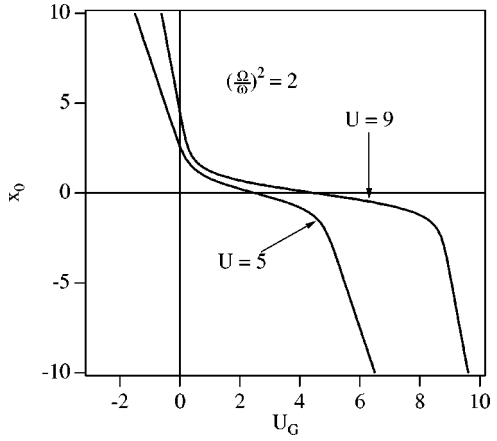

FIG. 6. The shift x_0 of nanoparticle vibration center versus the gate voltage for an asymmetrically applied source-drain voltage $U=5$ and 9 where $(\Omega/\omega)^2=2$.

-1), the slope of the pumped energy monotonically increases with increasing U. On the other hand, for $|\tilde{U}_G - U/2| \gg \frac{1}{2}(U-1)$, the slope of the pumped energy exponentially decays with increasing U or $|\tilde{U}_G|$, and hence nanoparticle vibrations are not anticipated even for very small γ. According to the argument for the intermediate voltage regions similar to the symmetric case, we have finally the conditions for the critical voltages $U_{G,C}$ and $U_{G,C'}$ for hysteretic nanoparticle vibrations

$$\frac{U-1}{2} < \left| \tilde{U}_{G,C(C')} - \frac{U}{2} \right| < \frac{U+1}{2} \tag{47}$$

as well as the number of electrons and holes carried by the nanoparticle as

$$N_e = \left\lfloor U - \tilde{U}_G + \frac{1}{2} \right\rfloor \geqslant 0, \tag{48}$$

$$N_h = \left\lfloor \tilde{U}_G + \frac{1}{2} \right\rfloor \geqslant 0. \tag{49}$$

Substituting

$$\tilde{U}_G = U_G + \frac{U}{2\varepsilon^*} \tag{50}$$

into conditions (48) and (49), we obtain the restriction on the electron and hole numbers as

$$N_e = \left\lfloor \left(1 - \frac{1}{2\varepsilon^*} \right) U - U_G + \frac{1}{2} \right\rfloor \geqslant 0, \tag{51}$$

$$N_h = \left\lfloor U_G + \frac{U}{2\varepsilon^*} + \frac{1}{2} \right\rfloor \geqslant 0. \tag{52}$$

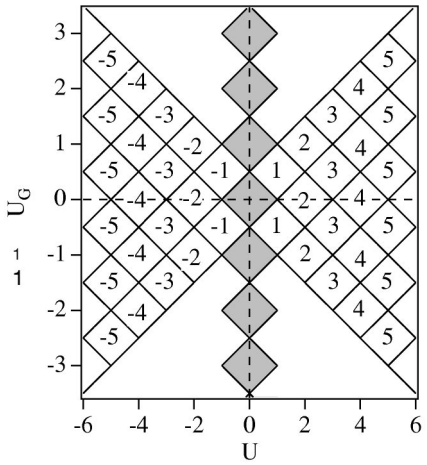

FIG. 7. Diagram of the current J in the (U,U_G) plane for symmetrically applied source-drain voltage. The shaded diamonds denote the voltage region where electron tunneling is prohibited at $T=0$ K.

IV. CURRENT-VOLTAGE CHARACTERISTICS

We investigate the dependence of the I-V characteristics on the gate voltage as well as the I-V_G characteristics for symmetrically and asymmetrically applied source-drain voltages.

A. Symmetric case

The current J per cycle can be obtained from Eqs. (4), (5), and (6):

$$J = \left\lfloor \frac{U}{2} - U_G + \frac{1}{2} \right\rfloor + \left\lfloor \frac{U}{2} + U_G + \frac{1}{2} \right\rfloor. \tag{53}$$

Obviously, J is an odd function of U, which increases by 2 for an increase of U by 2 at fixed U_G:

$$J(U+2,U_G) = J(U,U_G) + 2. \tag{54}$$

On the other hand, J is an even and periodic function of U_G:

$$J(U,U_G+1) = J(U,U_G), \tag{55}$$

where the change of N_e is compensated by that of N_h. At the same time, the current is subject to restrictions on N_e and N_h given by Eqs. (39) and (40).

In order to see the dependence of the current on both U and U_G, we draw a diagram denoting the expected current values for given U and U_G in Fig. 7, using Eqs. (39), (40), and (53). The number within each diamond denotes the sum of N_e and N_h. N_e or N_h differs by unity across an edge, and then the periodic increase of J with respect to U, from Eq. (54), becomes staircase structure. The periodic change of J with respect to U_G, from Eq. (55), shows switching between two current values with the change in U_G. But the periodic behavior of the current in Eqs. (54) and (55) are terminated by the critical voltages or the restriction on N_e and N_h, resulting in the butterfly-shape voltage region. We should note here that the edge for the butterfly-shape region of the

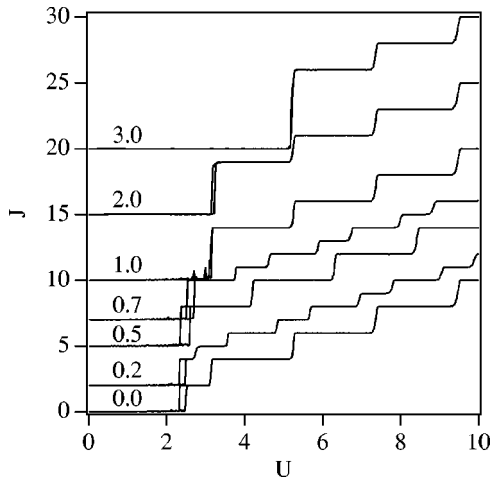

FIG. 8. *I-V* characteristics for U_G from 0 to 3 for symmetrically applied source-drain voltage by numerical simulation. The effect of confinement of the nanoparticle between the electrodes is taken into account in the simulations by using anharmonic potential in Eq. (7). Parameters used in the simulations are $\gamma\omega=0.1$, $\nu_R=0.01$, and $(\Omega/\omega)^2=2$. The *I-V* curves show staircase structure together with hysteresis with respect to the change in source-drain voltage. The voltages at which $\partial I/\partial V$ peaks appear are slightly shifted from those deduced from Fig. 7, because the term uU/ε^*L in Eq. (2) is taken into account in the simulations. See Ref. 5 for the details of the numerical simulations.

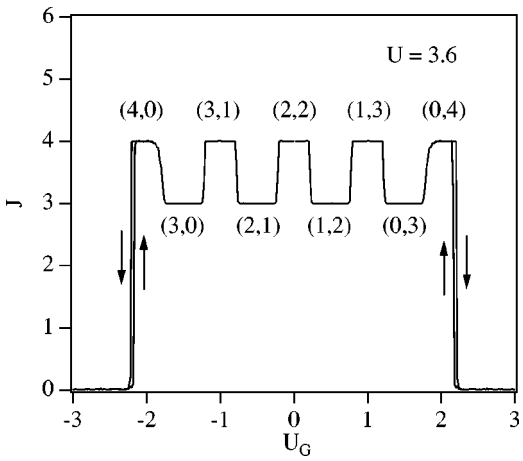

FIG. 9. Current versus the gate voltage for the symmetric case at $U=3.6$ by numerical simulation. The periodic change of the current, the drops as well as the hysteresis with respect to the change of the gate voltage, are visible. The numbers denote the electron and hole numbers (N_e,N_h) for each current level. Parameters used in the simulations are the same as those in Fig. 8.

voltages does not refer to critical voltages but indicates that the critical voltages should exist in the diamonds that include this edge. The shaded diamonds denote the region where tunneling is prohibited at $T=0$ K.[15] In the other regions the current is attributed only to the usual electron tunneling between the nanoparticle and the electrodes, whose magnitude, however, should be extremely small compared with that for the nanoparticle fixed at the center. This is because the tunneling rate across the less conductive barrier substantially decreases, by the factor of $e^{-L/2\lambda}\approx 5\times 10^{-5}$, due to the shift in the position of the nanoparticle to the vicinity of one of the electrodes, becoming a bottleneck for electron transport. Therefore, the current almost vanishes outside the butterfly-shape voltage region, resulting in the conduction gap. The voltage width of the conduction gap ΔU_{CG} is expressed as

$$\Delta U_{CG}\approx 4\left|\,|U_G|-\frac{1}{2}\right|, \tag{56}$$

which widens in proportion to the gate voltage.

The transport properties deduced above can be confirmed by means of numerical simulations. Here we use an algorithm described by Bakhvalov[11] for tunneling and a Symplectic Integrator[16] for nanoparticle motion. Figure 8 shows the *I-V* curves for several magnitudes of U_G from 0 to 3 for $\gamma/\omega=0.2$, $\nu_R=0.01$, and $(\Omega/\omega)^2=2$. The staircase *I-V* curves show staircase structure with the hysteresis behavior. The critical voltage increases with the increase of the gate voltage as expected from Fig. 7. The current steps at $U_G=0$ split apart into two steps moving to lower and higher voltages on increasing the gate voltage, and two steps merge into one when U_G becomes an integer or half-integer. This behavior agrees with that expected from Fig. 7. Figure 9 plots the current versus U_G at $U=3.6$, showing a periodic response with respect to U_G and a fall in the current as well as hysteretic behavior.

B. Asymmetric case

The current J per cycle yields

$$J=\left\lfloor\left(1-\frac{1}{2\varepsilon^*}\right)U-U_G+\frac{1}{2}\right\rfloor+\left\lfloor U_G+\frac{U}{2\varepsilon^*}+\frac{1}{2}\right\rfloor. \tag{57}$$

In contrast to the symmetric case, J does not support the periodic increase with an increase of U, but only the periodicity with respect to U_G, i.e., Eq. (55). This implies that the diagram for the current is not symmetric for inversion of the source-drain voltage or the gate voltage but instead is sheared, depending on ε^*. Figure 10 plots the rhombic diagram for the current value in the (U,U_G) plane, where we tentatively put $\varepsilon^*=3$.[8] The shaded rhombi denote the voltage regions where electron tunneling is prohibited, and the current outside the butterfly-shaped voltage region is expected to be negligibly small. The asymmetry of the diagram leads to asymmetric *I-V* characteristics except for $U_G=0$. At $U_G=0$, most of the current steps have a height of unity, irrespective of the gate voltage, unlike the symmetric case. Figure 11 shows a plot of the *I-V* curves with hysteresis for several gate voltages, evaluated by numerical simulation. The Coulomb staircase has current steps which periodically appear with respect to U, and the current step has a height of unity as deduced from Fig. 10. The *I-V* curves for $U_G=0$, 1, and 2 are the same except for the rise, which reflects the periodic dependence on the gate voltage. The periodic behavior of J and the hysteresis with the change in gate voltage are also confirmed in Fig. 12.

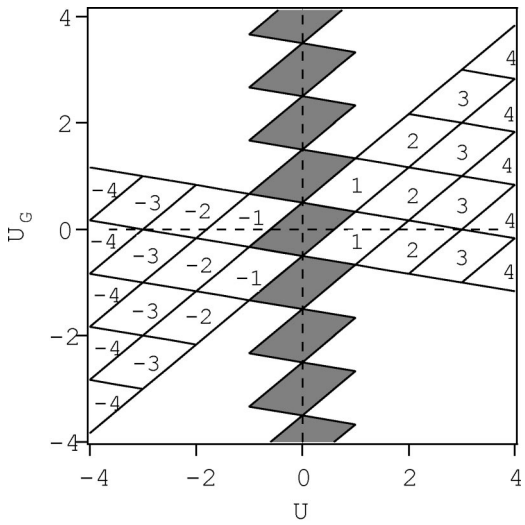

FIG. 10. The diagram of the current J in the (U, U_G) plane for asymmetrically applied source-drain voltage. The shaded rhombi denote the voltage region where electron tunneling is prohibited at $T=0$ K.

V. SUMMARY AND DISCUSSION

We have studied the effect of the gate voltage on the electron transport of a single-electron transistor using the shuttle mechanism, and demonstrated two types of significant effect on the transport: one is the direct modulation of the current due to the gate voltage, which appears as the split of the current steps and their shift with the change in gate voltage. In addition, periodic behavior of the current with respect to the gate voltage appears for fixed source-drain voltage; the other is an indirect effect through the shift in the region of the nanoparticle vibrations. The latter plays a crucial role in the transport, which not only suppresses electron tunneling between the nanoparticle and one of the electrodes from which the nanoparticle recedes, but also limits pumping of vibration energy via the electrostatic force by narrowing the vibration region. A substantial shift at a large value of the gate voltage stops the nanoparticle vibrations, resulting in a conduction gap which widens in proportion to the gate voltage. The voltage region for the shuttle current expands according to a butterfly shape in the source drain voltage–the gate voltage plane, from which we obtain the restriction on the electron or hole numbers at the critical voltages $N_e=0$ or $N_h=0$.

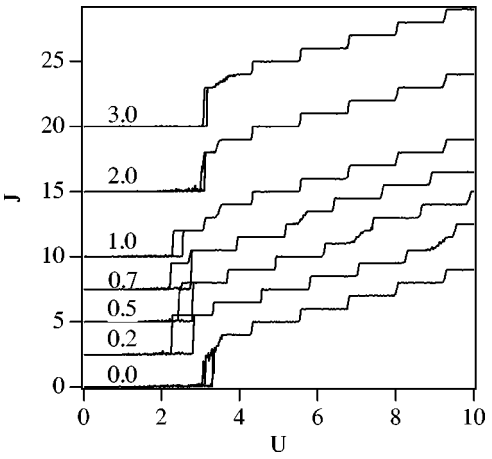

FIG. 11. *I-V* characteristics for U_G from 0 to 3 for asymmetrically applied source-drain voltage by numerical simulations. The simulation method is the same as for Fig. 8. The *I-V* curves show staircase structure together with hysteresis with respect to the change in the source-drain voltage. The slight disagreement of the voltages at which $\partial I/\partial V$ peaks appear with those deduced from Fig. 10 are due to the fact that the term uU/ε^*L in Eq. (2) is taken into account in the simulations, here.

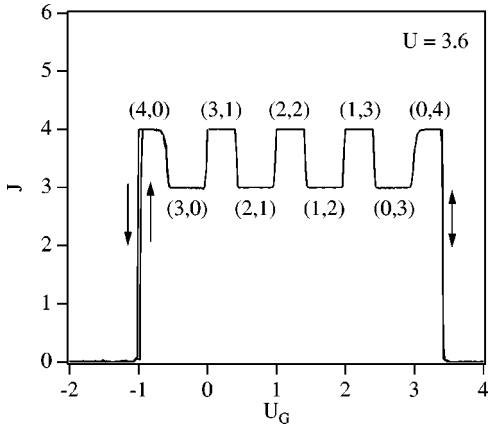

FIG. 12. Current versus gate voltage for the asymmetric case at $U=3.6$ by numerical simulation. The periodic change of the current, the drops as well as the hysteresis with respect to the change of the gate voltage, are visible. The numbers denote the electron and hole numbers (N_e, N_h) for each current level. Parameters used in the simulations are the same as those in Fig. 11.

We have shown that the butterfly-shape voltage region for the shuttle current reflects the symmetry of the source-drain voltage. However, the shape of the voltage region depends not only on the symmetry of the source-drain voltage but also on the equilibrium position of the nanoparticle. Although in this work we put the initial mechanical equilibrium position of the nanoparticle on the midpoint of the electrodes, it will actually be difficult in practice to put nanoparticles precisely on target. The equilibrium position may obey some distribution function. Considering the offset of the position represented by d from the midpoint of the electrodes, the gate voltage U_G will then be replaced by $U_G + (d/\varepsilon^*L)U$ as readily understood from Eq. (2). The corresponding current is

$$J=\left\lfloor\left(\frac{1}{2}-\frac{d}{\varepsilon^*L}\right)U-U_G+\frac{1}{2}\right\rfloor+\left\lfloor\left(\frac{1}{2}+\frac{d}{\varepsilon^*L}\right)U+U_G+\frac{1}{2}\right\rfloor, \tag{58}$$

for the symmetric case, and

$$J=\left\lfloor\left(1-\frac{1}{2\varepsilon^*}-\frac{d}{\varepsilon^*L}\right)U-U_G+\frac{1}{2}\right\rfloor + \left\lfloor\left(\frac{1}{2\varepsilon^*}+\frac{d}{\varepsilon^*L}\right)U+U_G+\frac{1}{2}\right\rfloor, \tag{59}$$

for the asymmetric case. The position d should differ from sample to sample, producing a sample-dependent butterfly shape of the voltage regions for the shuttle current. Such variously sheared butterfly-shaped voltage regions are reported in the experimental work on the C_{60} single electron transistor[10] together with a conduction gap which widens in proportion to the gate voltage. The experiment also indicated that the number of excess electrons on the C_{60} molecule at the critical voltage of the conduction gap is 0 or 1. This is all consistent with the findings of the present work. We therefore conclude that the effect of vibration region shift induced by the gate voltage is essential for describing the transport properties of Coulomb Blockade devices due to the shuttle mechanism.

ACKNOWLEDGMENTS

The author acknowledges Shinsuke Asari and Takashi Ogawa for helpful discussions. He also acknowledges Oliver B. Wright for his helpful comment on the manuscript.

APPENDIX

The frequency of the nanoparticle vibrations may generally differ from the natural frequency ω. Then, substituting

$$x(t)=\tilde{x}\sin\omega' t+x_0 \tag{A1}$$

into Eq. (7), we have

$$\gamma\frac{d\tilde{x}}{dt}=-(\omega^2-\omega'^2)\tilde{x}+\Omega^2 U\langle n(t)\sin\omega' t\rangle \tag{A2}$$

in addition to Eqs. (11) and (12). For the steady state, ω' is related to ω by

$$\omega'^2=\omega^2-\frac{\Omega^2 U}{\sqrt{E}}\langle n(t)\sin\omega' t\rangle. \tag{A3}$$

The relative frequency shift $\sqrt{\delta\omega^2}/\omega$ is evaluated by using Eq. (26) as

$$\frac{\sqrt{\delta\omega^2}}{\omega}=\frac{\Omega}{\omega}\left[\frac{\nu_R^2 U(U-1)}{1+4\,\nu_R^2}+\frac{\nu_R^2 U(U-1)}{4}\,\frac{(1-4\,\nu_R^2)}{(1+4\,\nu_R^2)^2}E\right]^{1/2} \tag{A4}$$

$$\approx\nu_R\frac{\Omega}{\omega}\sqrt{U(U-1)}\left(1+\frac{E}{8}\right). \tag{A5}$$

Then, provided $\nu_R(\Omega/\omega)\ll 1$, frequency deviation from the natural frequency is expected little.

[1] L.Y. Gorelik, A. Isacsson, M.V. Voinova, B. Kasemo, R.I. Shekhter, and M. Jonson, Phys. Rev. Lett. **80**, 4526 (1998).
[2] A. Isacsson, L.Y. Gorelik, M.V. Voinova, B. Kasemo, R.I. Shekhter, and M. Jonson, Physica B **255**, 150 (1998).
[3] M.T. Tuominen, R.V. Krotkov, and M.L. Breuer, Phys. Rev. Lett. **83**, 3025 (1999).
[4] M.P. Blencowe and M.N. Wybourne, Appl. Phys. Lett. **77**, 3845 (2000).
[5] N. Nishiguchi, Jpn. J. Appl. Phys. **40**, 1923 (2001).
[6] G. Schön and U. Simon, Colloid Sci. **273**, 1010 (1995).
[7] C.J. Kiely, J. Fink, M. Brust, D. Bethell, and D.J. Schiffrin, Nature (London) **396**, 444 (1998).
[8] M.N. Wybourne, L. Clarke, M. Yan, S.X. Cai, L.O. Brown, J.E. Hutchison, and J.F.W. Keana, Jpn. J. Appl. Phys. **36**, 7796 (1997).
[9] R.L. Whettern, J.T. Khoury, M.M. Alvarez, S. Murthy, I. Vezmar, Z.L. Wang, P.W. Stephens, C.L. Cleveland, W.D. Luedtke, and U. Landman, Adv. Mater. **8**, 428 (1996).
[10] H. Park, J. Park, A.K.L. Lim, E.H. Anderson, A.P. Alivisatos, and P.L. McEuen, Nature (London) **407**, 57 (2000).
[11] N.S. Bakhvalov, G.S. Kazacha, K.K. Likharev, and S.I. Serdyukova, Zh. Éksp. Teor. Fiz. **95**, 1010 (1989) [Sov. Phys. JETP **68**, 581 (1989)].
[12] L.S. Kuzmin and K.K. Likharev, Pisma Zh. Éksp. Teor. Fiz. **45**, 389 (1987) [JETP Lett. **45**, 495 (1987)].
[13] From the experimental work on the resistance between the electrodes (Ref. 17) and on the work function of C_{60} molecules (Ref. 14), and provided that the classical electromagnetic formula used for a macroscopic substance is available for nanoparticles, ν_R is found to be larger than 10^{-3} and $(\Omega/\omega)^2$ is inferred to be of the order of unity for C_{60} molecules.
[14] A.J. Maxwell, P.A. Brühwiler, D. Arvanitis, J. Hasselström, M.K.-J. Johansson, and N. Mårtensson, Phys. Rev. B **57**, 7312 (1998).
[15] D.K. Ferry and S.M. Goodnick, in *Transport in Nanostructures* (Cambridge University Press, 1997), Chap. 4.
[16] P.J. Channel and J.C. Scovel, Nonlinearity **3**, 231 (1990).
[17] H. Park, A.K.L. Lim, and A.P. Alivisats, Appl. Phys. Lett. **75**, 301 (1999).